Contract No:

This document was prepared in conjunction with work accomplished under Contract No. DE-AC09-08SR22470 with the U.S. Department of Energy (DOE) Office of Environmental Management (EM).

Disclaimer:

Proceedings of the ASME 2015 Pressure Vessels & Piping Conference
PVP2015
July 19-23, 2015, Boston, Massachusetts, USA

PVP2015-45935

DEVELOPMENT OF FLAW ACCEPTANCE CRITERIA FOR AGING MANAGEMENT OF SPENT NUCLEAR FUEL MULTIPLE-PURPOSE CANISTERS

Poh-Sang Lam
Materials Science and Technology
Savannah River National Laboratory
Aiken, SC 29808, USA
ps.lam@srnl.doe.gov

Robert L. Sindelar
Materials Science and Technology
Savannah River National Laboratory
Aiken, SC 29808, USA
robert.sindelar@srnl.doe.gov

ABSTRACT

A typical multipurpose canister (MPC) is made of austenitic stainless steel and is loaded with spent nuclear fuel assemblies. The canister may be subject to service-induced degradation when it is exposed to aggressive atmospheric environments during a possibly long-term storage period if the permanent repository is yet to be identified and readied. Because heat treatment for stress relief is not required for the construction of an MPC, stress corrosion cracking may be initiated on the canister surface in the welds or in the heat affected zone. An acceptance criteria methodology is being developed for flaw disposition should the crack-like defects be detected by periodic Inservice Inspection. The first-order instability flaw sizes has been determined with bounding flaw configurations, that is, through-wall axial or circumferential cracks, and part-through-wall long axial flaw or 360° circumferential crack. The procedure recommended by the American Petroleum Institute (API) 579 Fitness-for-Service code (Second Edition) is used to estimate the instability crack length or depth by implementing the failure assessment diagram (FAD) methodology. The welding residual stresses are mostly unknown and are therefore estimated with the API 579 procedure. It is demonstrated in this paper that the residual stress has significant impact on the instability length or depth of the crack. The findings will limit the applicability of the flaw tolerance obtained from limit load approach where residual stress is ignored and only ligament yielding is considered.

INTRODUCTION

One of the options to close the nuclear fuel cycle is to dispose of the spent nuclear fuel in a permanent geological repository. However, before the repository is identified and approved for use, the continued safe storage until final disposition of the spent nuclear fuel (SNF) is a challenge to the nuclear industry. The SNF are initially stored in storage pools and then transferred to dry cask storage after sufficient time to allow cooling via radioactive decay. The present licensing basis for dry cask storage is up to 60 years (20-year initial license and 40-year re-license) but longer storage times may become necessary as the U.S. Department of Energy (DOE) and the U. S. Nuclear Regulatory Commission (NRC) evaluate repository options in a once-through strategy, and/or reprocessing options under modified open cycle or full recycle strategies. In clarification of the regulatory basis for continued storage, the NRC has recently established the rule for Continued Storage of Spent Nuclear Fuel [1] that will allow, in principle, re-licensing of storage systems for many additional decades.

Many Independent Spent Fuel Storage Installations (ISFSIs) are located near the coastal regions. Because the stainless steel canisters in these dry storage systems were not stress relieved for the welding residual stress, the chloride induced stress corrosion cracking (CISCC) might take place under marine salt and other atmospheric deposit contaminants [2-12]. If the cracking approaches the instability crack size, it will compromise the safety-credited containment boundary of the storage system such as the multipurpose canisters (MPC).

The NDE (non-destructive evaluation) or NDT, (non-destructive testing) techniques are being developed to deploy sensors through the narrow annular space in the dry cask system to detect service-induced planar and non-planar flaws (e.g., cracking and pitting) on the surface of the canister. Flaw acceptance criteria are needed for the disposition of the inspection results should relevant indications be found. Recently, an attempt to develop the instability crack lengths and depths was reported for, respectively, through-wall and part-through-wall cracks [13]. The analysis was based on ASME Boiler and Pressure Vessel Code Section XI [14] with a limit load approach which depends on the material's minimum tensile properties of the steel as provided by the ASME Section II [15]. The welding residual stress was not considered.

In the previous paper [16], the development of a fracture mechanics-based flaw disposition protocol to establish the flaw acceptance criteria for these canisters was outlined. The API 579 codified procedure for Fitness-for-Service [17] with the failure assessment diagram (FAD) methodology is adopted in the current analysis. The welding residual stresses for the longitudinal (axial) and circumferential (girth) welds, respectively, are estimated based on API 576 recommendation since the welding parameters are proprietary information and hence are not available for this analysis. For a direct comparison of the flaw tolerance results, the loading conditions, tensile properties (Type 304 stainless steel), and the (bounding) flaw configurations are selected identically to those in Reference [13]. The geometry of the Holtec HI-STORM canister [18,19] is used for the current work. Because the FAD is used in the development, the fracture toughness (K_{IC}) of the material is needed and is based on API 579 recommendation with a reference to the material test data obtained under the Savannah River Reactor Materials Program [20].

It was found that with the residual stress included as part of the loading, and with the consideration of elastic-plastic fracture mechanics through the FAD formulation, the resulting instability crack sizes have been significantly reduced from those based on the net section yielding limit load approach. The results are reported in this paper.

CONSTRUCTION AND LOADING OF MPC

Various canister designs have been used to store fuel at ISFSIs. In the present work, a typical cask system, Holtec International Storage Module, (HI-STORM) [18,19] is selected for the calculation of instability crack sizes in the development of acceptance criteria for structural integrity assessment. This MPC is a cylindrical shell with all components made of austenitic stainless steel (Typically, 304 stainless steel) [18]. The height of the canister is 4.8 m (15.8 ft) with an outer diameter 1.73 m (5.7 ft) and the thickness of the shell is 1.27 cm (0.5 in.).

The cylindrical shell is constructed with a circumferential (girth) weld in the mid-height and four axial seam welds (Fig. 1). The upper and lower axial welds are offset slightly along the circumferential weld. The shell is welded to a bottom plate with a thickness of 6.35 cm (2.5 in.) [18]. The submerged arc welding (SAW) with full penetration is applied. Although the post-weld nondestructive inspection is carried out, the heat treatment to relieve the welding residual stress is not required for the construction. The flaw acceptance criteria will be developed for postulated flaws in the heat affected zone (HAZ) in these critical locations.

The fuel assemblies are loaded vertically into HI-STORM canister. The total weight of the loaded canister is about 36 metric tons or 40 tons (see Table 1). The closure welds in the lid region were not considered in the MPC failure assessment [1] because 1) the tungsten inert gas (TIG) welds in the lid region are tougher than the submerged arc welds in the canister shell and the baseplate; 2) the multiple layers of welds (between the closure ring and shell; and between the lid and shell) provide redundant safety features for the lid, and 3) the lower stresses are expected in the lid. Therefore, the flaw acceptance criteria are not developed for closure welds.

The loading conditions that are used to develop the flaw acceptance criteria by calculating the instability crack sizes are listed in Table 1. Both normal and accident conditions are included, and are identical to those employed in a previous flaw tolerance analysis [15] based on limit load [14].

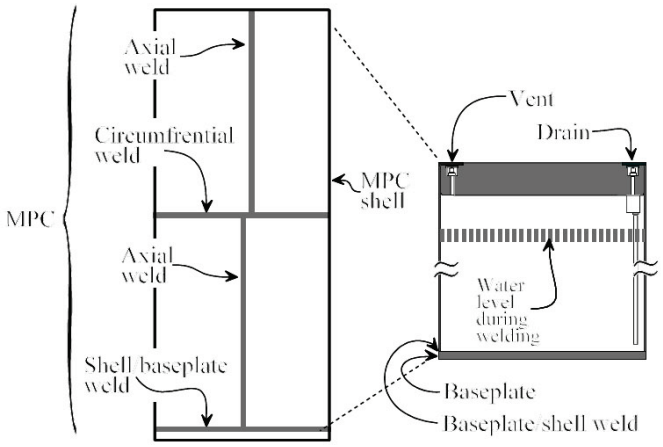

FIGURE 1 WELDS ON A MULTIPURPOSE CANISTER (REPRODUCED FROM NUREG-1864 [18], FIG. 16)

TABLE 1 LOAD CASES FOR CANISTER HI-STORM

Loading Case	Design Internal Pressure [MPa (psig)]	Loaded Canister Mass [kg (kips)]	Axial Handling Load or Acceleration
Normal	0.69 (100)	40800 (90)	1.15g
Accident	1.38 (200)	40800 (90)	1.15g

FRACTURE METHODOLOGY

The initiation and growth of the stress corrosion cracking, in particular, CISCC, on the external surface of the austenitic stainless steel canister in the HAZ is elastic-plastic in nature. The welding residual stress is expected to play an important role in the subcritical crack growth until the instability length (for a through-wall flaw) or depth (for a part-through-wall flaw) is reached. To include all the contributory factors in the development of flaw disposition technology, it appears that API 579-1/ASME FFS-1, Fitness-For-Service code [17] is an appropriate choice. It is emphasized that citation of this code does not imply that it is the adopted code of record for flaw disposition for the canisters at ISFSIs.

The API 579 recommends that Level 3 Assessment be used if subcritical crack-growth is possible during the structural component is in service. However, Level 3 Method A Assessment requires the use of Level 2 Assessment procedure and the FAD with *user specified* Partial Safety Factors based on a risk assessment, which, unfortunately, are unavailable for the current analysis. It is decided that Level 2 Assessment is conducted to establish the flaw acceptance criteria, and to defer the extra requirements to meet Level 3 Assessment (e.g., *user specified* Partial Safety Factors) for future work, or to properly adjust the inspection results when the indication is found by inservice inspection. Note that the code-defined Partial Safety Factors are provided in API 579 Part 9 *Assessment of Crack-like Flaws*, but are not to be applied to the current analysis for the same reason. This deviation from the code allows a direct comparison of the results between the API 579 FAD approach and the limit load approach reported in Reference [13], where the safety factors were not applied.

The main components of API 579 approach are the determination of the welding residual stress and the formulation of the failure assessment diagram. They are discussed in the following sub-sections.

Welding Residual Stress

Four flaw configurations (Figs. 2 to 5) in the HAZ are considered for developing the MPC acceptance criteria: 1) Axial crack parallel to an axial (or longitudinal) weld with dominant residual stress perpendicular to the weld (to open the crack), 2) Axial crack perpendicular to a circumferential (girth) weld with dominant residual stress parallel to the weld, 3) circumferential crack parallel to an circumferential weld with dominant residual stress perpendicular to the weld, and 4) circumferential crack perpendicular to an axial weld with dominant residual stress parallel to the weld. All the responsible residual stresses can be estimated by API 579 if the actual measurement or numerical simulation is not available. The major input for the calculations in API 579 Annex E *Residual Stress in a Fitness-for-Service Evaluation* includes the following:

1. Yield Stress – If no actual yield strength is available, then the yield stress used to estimate the residual stress is $\sigma_{ys}^{r} = \sigma_{ys} + 69\ MPa$ (or $\sigma_{ys}^{r} = \sigma_{ys} + 10\ ksi$), where σ_{ys}^{r} is the magnitude of the effective yield strength used to estimate the residual stress, and σ_{ys} is the specified minimum yield strength of the material. This 69 MPa elevation from the minimum yield strength is to account for the actual material properties, which are typically higher than the code minimum requirements. From ASME Boiler and Pressure Vessel Code, Section II, Part D, [15], the minimum yield strength listed in its Table 1A for 304 stainless steel is 205 MPa (30 ksi) and the minimum tensile strength (UTS) is 515 MPa (75 ksi). Note that for the current analysis with API 579 Level 2 (also Level 3) Assessment [17], the flow stress, and thus the UTS, is not used. Also note that the maximum temperature limit for using these properties is 427 °C (800 °F) for ASME Section III Classes 2 and 3 pressure vessels.
2. Welding Parameters – API 579 Annex E "*Residual Stresses in a Fitness-for-Service Evaluation*" [17] provides estimation equations for calculating the membrane and bending components of the residual stress. The heat input density parameter ($\hat{Q}$), which is a function of linear heat input to the weld $\dot{q} = (IV\eta)/u$, where I is the welding current, V is the welding voltage, and η is welding arc efficiency, and u is the welding travel speed. However, these parameters are proprietary information and are not for public assimilation. Therefore, the API 579 Annex E [17] suggested value for SAW average heat input 1080 J/mm is selected for analysis. This average heat input was based on 4 mm electrode, 889 mm/min travel speed, with 500A-32V for stainless steel. The code also provides the upper bound heat input 1920 J/mm based on 750A-38V, but is not used in the current work. In addition, the weld joint configuration also affects the residual stresses. In this study, the double-V notch was assumed.

With the effective yield stress and the welding parameters given above, the estimated residual stresses through the thickness of the canister shell for the four flaw configurations are shown in Figures 2 to 5. Each of the residual stress (RS) distribution is also fitted with a fourth-order polynomial, from which its coefficients are useful for calculating the stress intensity factor based on API 579 Part 9 [17]. These coefficients may also be used for calculating the reference stress, but the membrane and bending parts of the residual stress are often used. Note that the coordinate (x) in the fourth-order polynomial is reversed with respect to Figures 2 to 5 due to the sign convention for flaws on the outside surface of the canister. Table 2 shows the form and the coefficients of the polynomial.

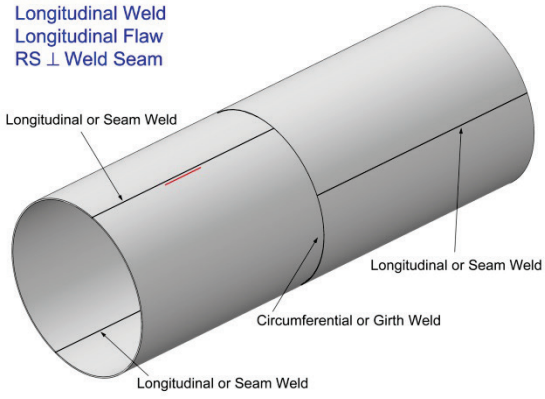

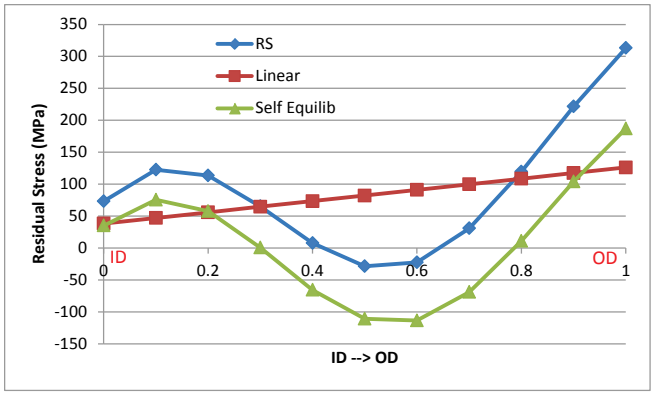

FIGURE 2 CASE 1: AXIAL CRACK PARALLEL TO AN AXIAL WELD - RESIDUAL STRESS PERPENDICULAR TO THE AXIAL WELD WITH A DOUBLE-V NOTCH

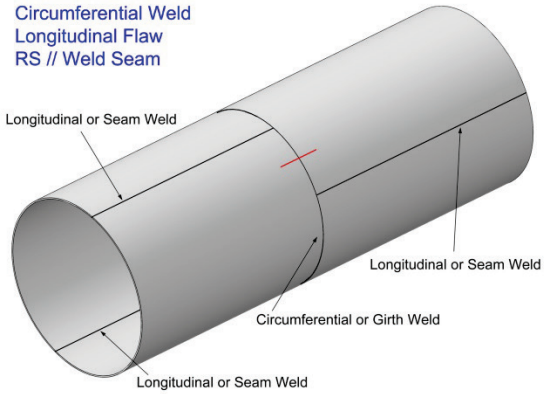

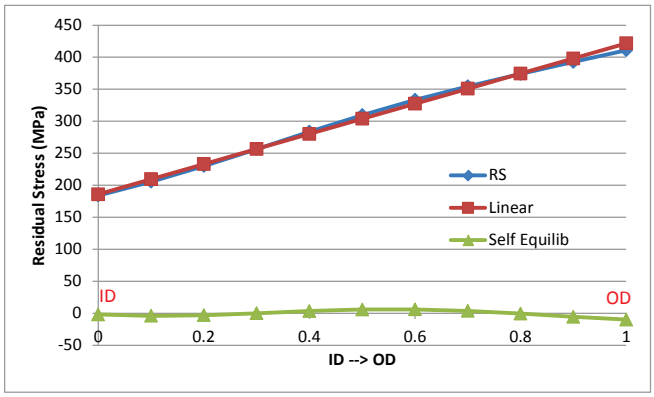

FIGURE 3 CASE 2: AXIAL CRACK PERPENDICULAR TO A CIRCUMFERENTIAL WELD - RESIDUAL STRESS PARALLEL TO THE CIRCUMFERENTIAL WELD WITH A DOUBLE-V NOTCH

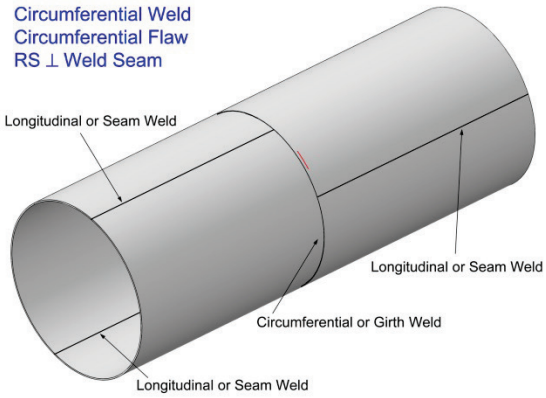

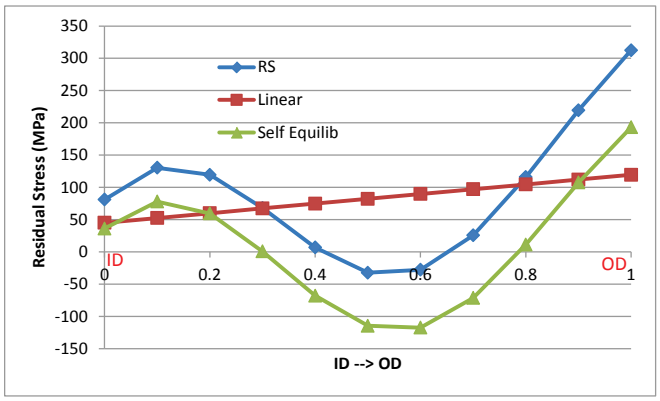

FIGURE 4 CASE 3: CIRCUMFERENTIAL CRACK PARALLEL TO A CIRCUMFERENTIAL WELD - RESIDUAL STRESS PERPENDICULAR TO THE CIRCUMFERENTIAL WELD WITH A DOUBLE-V NOTCH

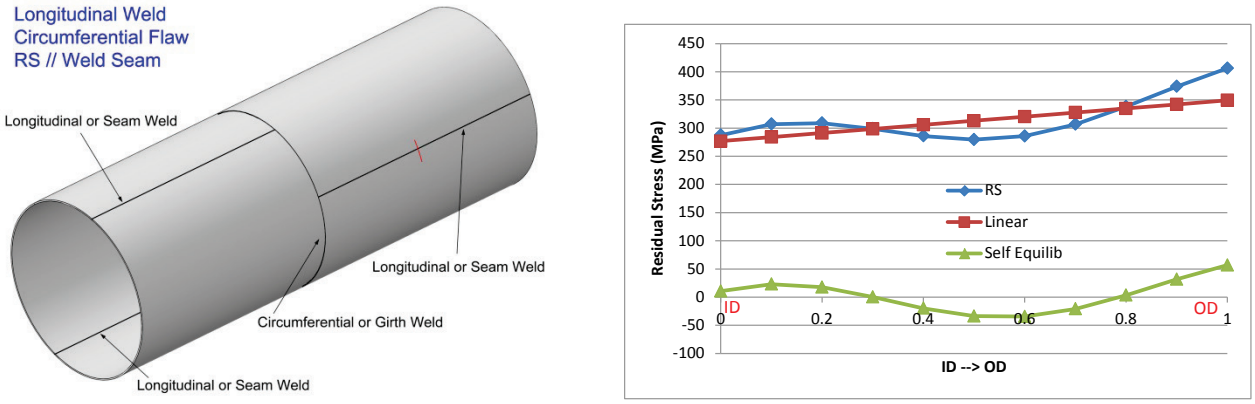

FIGURE 5 CASE 4: CIRCUMFERENTIAL CRACK PERPENDICULAR TO AN AXIAL WELD - RESIDUAL STRESS PARALLEL TO THE AXIAL WELD WITH A DOUBLE-V NOTCH

TABLE 2 COEFFICIENTS OF THE FOURTH ORDER POLYNOMIAL FOR THOUGH-THICKNESS RESIDUAL STRESS (σ^R)

$$\sigma^R = \sigma_0 + \sigma_1\left(\frac{x}{t}\right) + \sigma_2\left(\frac{x}{t}\right)^2 + \sigma_3\left(\frac{x}{t}\right)^3 + \sigma_4\left(\frac{x}{t}\right)^4$$

(x=0 at the outside surface and x= t at the inside surface)

Case	σ_0 (MPa)	σ_1 (MPa)	σ_2 (MPa)	σ_3 (MPa)	σ_4 (MPa)
1	314.60	-790.83	-2248.35	7081.99	-4288.01
2	410.99	-190.54	91.54	-339.02	211.26
3	314.13	-800.73	-2323.15	7317.54	-4430.58
4	406.69	-286.26	-683.33	2152.36	-1303.24

Note: Outside surface: x= 0
Inside Surface: x= t, where t is the wall thickness

Failure Assessment Diagrams (FAD)

The traditional failure assessment diagram (FAD) [21] is a crack growth resistance curve in terms of L_r (abscissa) and K_r (ordinate), where the stress ratio L_r is defined as the ratio of the applied load (P) to a reference load (P_o), which is the limit load based on net section yielding. To reflect better material behavior under strain hardening, Ainsworth [22] redefined L_r by introducing a reference stress from the primary load as $\sigma_{ref}^p = (P/P_0)\sigma_{ys}$, where σ_{ys} is the yield stress of the material. Therefore, the abscissa for the FAD becomes

$$L_r^P = \frac{\sigma_{ref}^p}{\sigma_{ys}}$$

API 579 also suggests a modified form for the ordinate of the FAD (K_r). A plasticity interaction factor $\mathbf{\Phi}$ is estimated as a function of L_r^P (the L_r value defined above for the primary load) and L_r^{SR} (the L_r value based on the secondary load, which in the current case is the residual stress). The details can be found in API 579 Part 9 [17]. The modified form for the ordinate is

$$K_r = \frac{K_I^P + \mathbf{\Phi} K_I^{SR}}{K_{mat}}$$

where K_I^P is the stress intensity factor from the primary load, K_I^{SR} is the stress intensity factor from the secondary load (e.g., residual stress), and K_{mat} is the fracture toughness of the material.

The values of reference stress σ_{ref}^p and the stress intensity factor K_I^P from the primary load are calculated according to the loading conditions given in Table 1 with the formulae provided by API 579 (primarily from Part 9, Annexes C and D) [17]. The values of L_r^{SR} and K_I^{SR} are calculated based on, for the current analysis, the residual stress distributions across the thickness of the canister shell in previous subsection of this paper and the equations in API 579.

The yield stress of the material for this analysis uses the ASME minimum yield strength for 304 stainless steel 205 MPa (30 ksi) [15] as discussed earlier. A comprehensive testing for stainless steel piping systems was carried out under the Savannah River Reactor Materials Program in early 1990. The room temperature and 125 °C data for the tensile, Charpy, and fracture toughness of the base metal, weld metal and the HAZ along C-L and L-C directions were reported for Type 304 stainless steel large diameter piping joined with Type 308 stainless steel weld filler [20]. The lowest fracture toughness at 125 °C for the HAZ is K_{JC}= 207 MPa$\sqrt{\text{m}}$, where K_{JC} is converted from J_{IC} obtained from the J-R curve testing with 0.394T-CT specimens in C-L direction. However, at that temperature only two samples were tested and the data range was large: 175-239 MPa$\sqrt{\text{m}}$. Therefore, the fracture toughness for the current FAD analysis adopts the recommendation from API 579 Annex F "*Materials Properties for a FFS Assessment*," Paragraph 4.8.2 [17], from which the base metal K_{mat} = 220 MPa$\sqrt{\text{m}}$ (or 200 ksi$\sqrt{\text{in}}$) is chosen since the flaws are assumed to be initiated in the HAZ.

The API 579 Level 2 and Level 3 Method A Assessment (in Part 9) [17] use the following assessment curve to define the instability flaw size:

$$K_r = [1 - 0.14(L_r^P)^2]\{0.3 + 0.7\ exp[-0.65(L_r^P)^6]\} \quad (1)$$

for $L_r^P \le L_{r(max)}^P$. For austenitic stainless steels, the maximum permitted value (or cut-off value) of L_r^P is $L_{r(\max)}^P = 1.8$. Figure 6 is the FAD used in the current work for calculating the instability crack size with API 579 Level 2 Assessment methodology.

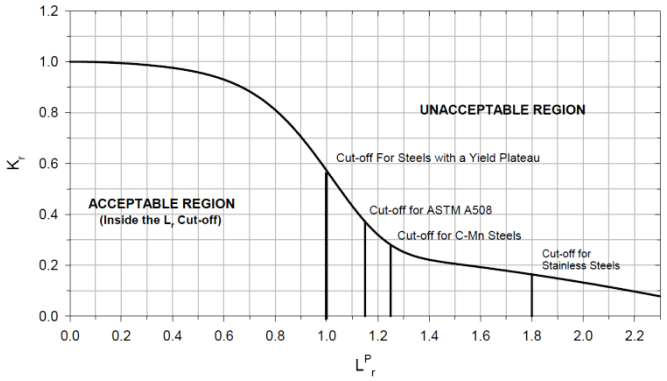

FIGURE 6 TYPICAL FAILURE ASSESSMENT DIAGRAM (REPRODUCED FROM API 579 Part 9 FIG. 9.20 [17])

Instability Crack Size

Only bounding flaws are considered in the present work, that is, 1) part-though-wall very long axial crack, part-though-wall 360° circumferential crack, through-wall axial crack, and through-wall circumferential crack. They are all assumed to initiate in the HAZ near the weld. The instability crack sizes (depth or length) are calculated with the given loading conditions in Table 1. For each of the flaw configuration and its relative location with respect to the neighboring weld can be seen in Figures 2 to 5. The flaw size is gradually increasing with a fixed set of loading until the corresponding assessment point ($L_r^P - K_r$ pair) falls exactly on the faliure assessment curve (Eq. 1). This approach is very similar to the development of acceptance criteria for DOE Savannah River Site high level nuclear waste tanks by Lam [23] and by Lam and Sindelar [24].

The flaw size such obtained is defined as the instability crack length or depth. The results are summarized in Tables 3 to 6. The previouisly published flaw tolerance using limit load or net section yielding approach [13] is also included in these tables for comparison purpose. A significant reduction in the instability crack size can be seen by the inclusion of welding residual stress in the calculation with the FAD formulation.

TABLE 3 INSTABILITY CRACK LENGTH (2*c*): THROUGH-WALL AXIAL CRACK (UNITS: mm)

	EPRI [13] (based on Limit Load)	FAD (No Residual Stress)	FAD (Axial Crack // Axial Weld)	FAD (Axial Crack ⊥ Circumferential Weld)	Crack Tip Location
Normal	1200	730 (outside)	334* (outside)	128 (outside)	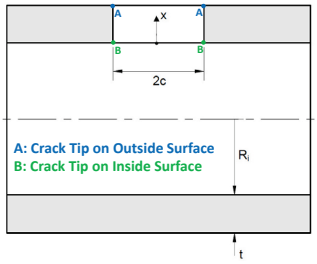
		690* (inside)	338 (inside)	118* (inside)	
Accident	600	334* (outside)	226* (outside)	102 (outside)	
		350 (inside)	234 (inside)	88* (inside)	
Crack Configuration	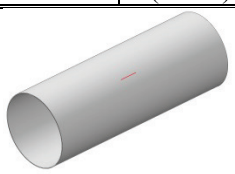	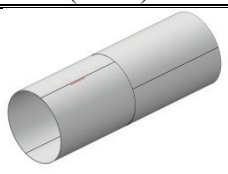	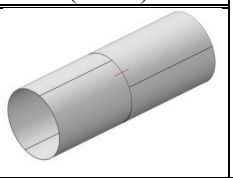		

Note: A "*" denotes the limiting instability crack length for each of the crack-weld configuration.

TABLE 4 INSTABILITY CRACK LENGTH (2*c*): THROUGH-WALL CIRCUMFERENTIAL CRACK (UNITS: mm)

	EPRI [13] (based on Limit Load)	FAD (No Residual Stress)	FAD (Circumf. Crack // Circumf. Weld)	FAD (Circumf. Crack ⊥ Axial Weld)	Crack Tip Location
Normal	3300	1543 (outside)	614 (outside)	160* (outside)	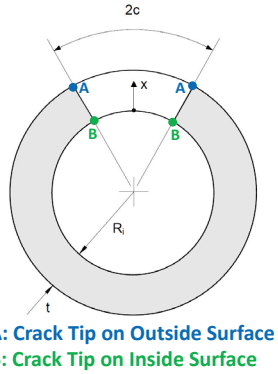
		1124* (inside)	554* (inside)	180 (inside)	
Accident	2800	1079 (outside)	255 (outside)	141* (outside)	
		860* (inside)	241* (inside)	156 (inside)	
Crack Configuration	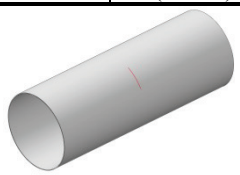		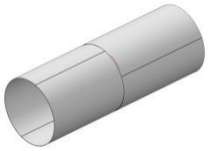	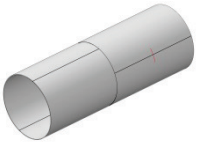	

Note: A "*" denotes the limiting instability crack length for each of the crack-weld configuration.

TABLE 5 INSTABILITY CRACK DEPTH (*a*/*t*): PART THROUGH-WALL LONG AXIAL CRACK

	EPRI [13] (based on Limit Load)	FAD (No Residual Stress)	FAD (Axial Crack // Axial Weld)	FAD (Axial Crack ⊥ Circumferential Weld)	Cracked Cross-section
Normal	86%	80%	70%	51%	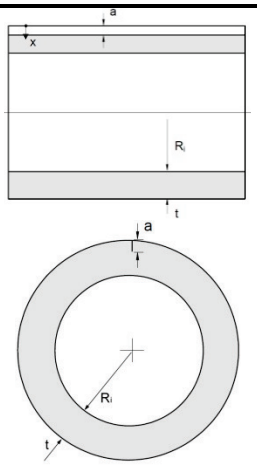
Accident	73%	63%	57%	43%	
Crack Configuration	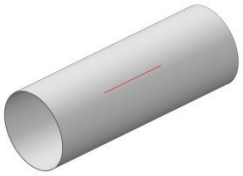		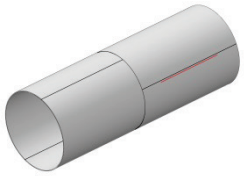	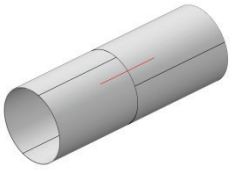	

TABLE 6 INSTABILITY CRACK DEPTH (*a*/*t*): PART THROUGH-WALL 360° CIRCUMFERENTIAL CRACK

	EPRI [13] (based on Limit Load)	FAD (No Residual Stress)	FAD (Circumf. Crack // Circumf. Weld)	FAD (Circumf. Crack ⊥ Axial Weld)	Cracked Cross-section
Normal	91%	92%	>80% (Exceed limit for valid elastic solution)	61%	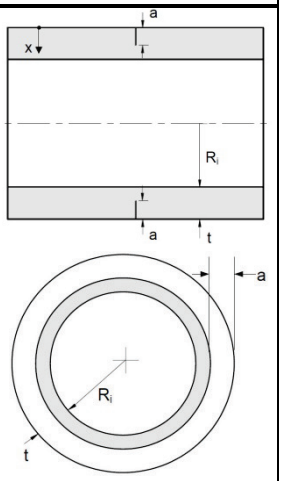
Accident	84%	83%	76%	56%	
Crack Configuration	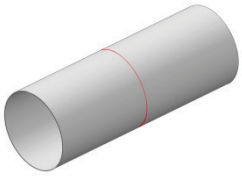	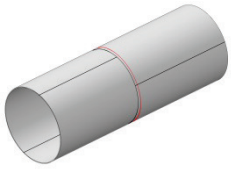	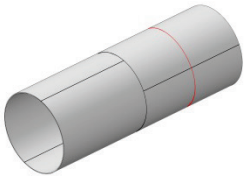		

FLAW ACCEPTANCE METHODOLOGY

The flowchart representing a general approach for the flaw disposition acceptance criteria is shown in Figure 7. It should be noted that, when the depth (a) of a part-through-wall crack exceeds certain fraction of the shell thickness (t), the crack should be recategorized as a through-wall crack due to the uncertainties in sizing, and the high stress intensity at the crack tip leading to uncertainties in the elastic fracture mechanics evaluation to justify stability. When this occurs, the requirement for the through-wall instability crack length ($2c$) must be met. This limit of applicability for the part-through-wall crack is tentatively set to a/t= 0.8, beyond which the elastic solution for the stress intensity factor becomes invalid. The frequency for inservice inspection will depend on the amount of subcritical crack growth, but it is outside the scope of the present work.

SUMMARY AND PATH FORWARD

Tables 3 to 6 summarize the instability crack sizes developed in the current work. The results show significant effects from the welding residual stress, as well as the orientation of the crack with respect to the weld. It was found that the most limiting lengths for a through-wall axial crack are 118 mm (normal) and 88 mm (accident), only about 10% of the values proposed earlier [13]. Similarly, for a through-wall circumferential crack, the most limiting lengths are 160 mm (normal) and 141 mm (accident), and are about 5% of the earlier reported values. These crack lengths correspond to very small crack angles about 10°. These new estimates of the instability crack lengths severely limit the flaw tolerance when the flaw penetrates the shell thickness and becomes through-wall. For part-through-wall flaws, the severity may be less impacted. The most limiting crack depths for a very long part-though-wall axial crack are 51% and 43% of the shell thickness, respectively, for normal and accident conditions. These values are about 60% of the previously proposed values. In the case of a part-though-wall circumferential crack around the entire canister (360°), the most limiting crack depths are 61% (normal) and 56% (accident) of the shell thickness. They are about 70% of the values based on net section yielding without the consideration of residual stress.

For a more accurate flaw acceptance technology, semi-elliptic cracks should be used to calculate the instability crack size. Because of more parameters are needed to define the crack front geometry, the calculations based on API 579 become much more complicated but are still feasible. In addition, it has been shown that the residual stress cannot be neglected; more information on the weld geometry (such as single- or double-V notches) and the welding parameters (such as the electric current, voltage, and electrode travel speed) should be made available for a more realistic estimate. Finally, the loadings must be clearly defined for various types of canisters, and the canister-specific acceptance criteria should be developed.

ACKNOWLEDGEMENT

This work at the Savannah River National Laboratory was sponsored by the Nuclear Fuel Storage and Transportation (NFST) Planning Project under the U.S. Department of Energy, Office of Nuclear Energy; and by the Savannah River

Nuclear Solutions, LLC under Contract No. DE-AC09-08SR22470 with the U.S. Department of Energy.

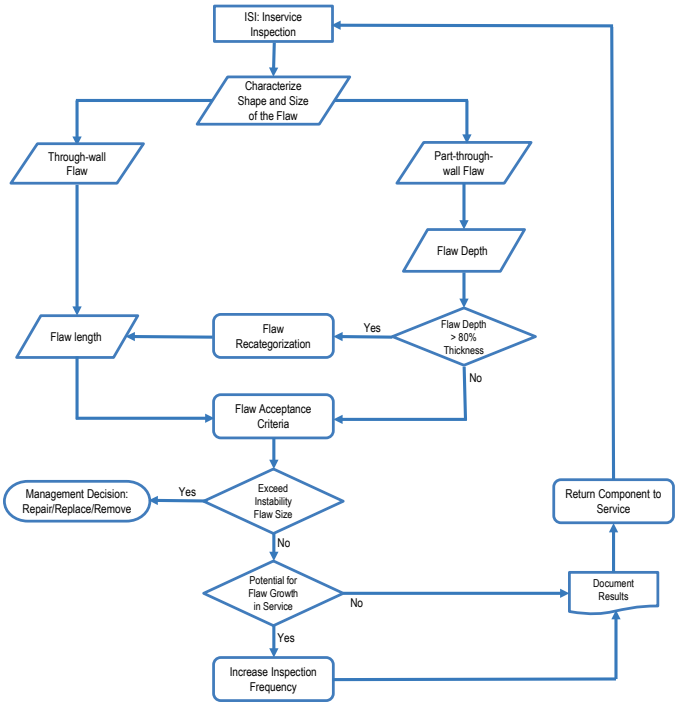

FIGURE 7 FLAW ACCEPTANCE CRITERIA PROPOSED FOR MULTI-PURPOSE CANISTER (MPC)

REFERENCES

[1] U. S. NRC, 2014, *Continued Storage of Spent Nuclear Fuel*, Federal Registry, Vol. 79, No. 182/Friday September 19, 2014/Rules and Regulations, United States Government, Washington, DC., USA.

[2] Kosaki, A., 2005, "The corrosion behavior of one-fifth scale lid models of transport cask submerged in sea bottom," Corrosion Science, 47, pp. 2361–2376.

[3] Kosaki, A., 2006, "SCC Propagation Rate of Type 304, 304L Steels under Oceanic Air Environment," Paper No. ICONE14-89271, Vol. 1, Plant Operations, Maintenance and Life Cycle; Component Reliability and Materials Issues; Codes, Standards, Licensing and Regulatory Issues; Fuel Cycle and High Level Waste Management, International Conference on Nuclear Engineering, July 17-20, Miami, Florida, USA, pp. 443-450

[4] J. Tani, Mayuzumi, M., Arai, T., and Hara, N., 2007, "Stress Corrosion Cracking Growth Rates of Candidate Canister Materials for Spent Nuclear Fuel Storage in Chloride-Containing Atmosphere," Materials Transactions, Vol. 48, No. 6, pp. 1431 to 1437.

[5] Kosaki, A., 2008, "Evaluation method of corrosion lifetime of conventional stainless steel canister under oceanic air environment," Nuclear Engineering and Design, 238, pp. 1233–1240.

[6] Tani, J., Mayuzumi, M., and Hara, N., 2008, "Stress corrosion cracking of stainless-steel canister for concrete cask storage of spent fuel," Journal of Nuclear Materials 379, pp. 42–47.

[7] Tani, J.I., 2009, "Initiation and Propagation of Stress Corrosion Cracking of Stainless Steel Canister for Concrete Cask Storage of Spent Nuclear Fuel," Corrosion, Vol. 65, No. 3, pp. 187-194.

[8] Caseres, L. and Mintz, T.S., 2010, Atmospheric Stress Corrosion Cracking Susceptibility of Welded and Unwelded 304, 304L, and 316L Austenitic Stainless Steels Commonly Used for Dry Cask Storage Containers Exposed to Marine Environments, NUREG/CR-7030, Office of Nuclear Regulatory Research, U.S. Nuclear Regulatory Commission, Washington, D.C., USA.

[9] Shirai, K., Tani, J. ,and Saegusa, T., 2011, "Study on Interim Storage of Spent Nuclear Fuel by Concrete Cask for Practical Use -Feasibility Study on Prevention of Chloride Induced Stress Corrosion Cracking for Type 304L Stainless Steel Canister," CRIEPI N10035, Central Research Institute of Electric Power Industry , Tokyo, Japan (In Japanese).

[10] Oberson, G., Dunn, D., Mintz, T., He, X., Pabalan, R., and Miller, L., 2013, "US NRC-Sponsored Research on Stress Corrosion Cracking Susceptibility of Dry Storage Canister," Materials in Marine Environments – 13344, WM2013 Conference, February 24 – 28, 2013, Phoenix, Arizona USA.

[11] He, X., Mintz, T. S., Pabalan, R., Miller, L., and Oberson, G., 2014, Assessment of Stress Corrosion Cracking Susceptibility for Austenitic Stainless Steels Exposed to Atmospheric Chloride and Non-Chloride Salts, NUREG/CR-7170, Office of Nuclear Regulatory Research, U.S. Nuclear Regulatory Commission, Washington, D.C., USA.

[12] Chopra, O.K., Diercks, D.R., Fabian, R.R., Han, Z.H. and Liu, Y.Y., 2014, Managing Aging Effects on Dry Cask Storage Systems for Extended Long-Term Storage and Transportation of Used Fuel, Rev. 2," FCRD-UFD-2014-000476, ANL-13/15, U.S. Department of Energy, Washington, D.C., USA.

[13] Chu, S., 2014, *Flaw Growth and Flaw Tolerance Assessment for Dry Cask Storage Canisters*, No. 3002002785, Electric Power Research Institute, Palo Alto, CA., USA.

[14] ASME Boiler and Pressure Vessel Code, Section XI, *Rules for Inservice Inspection of Nuclear Power Plant Components*, 2013, American Society of Mechanical Engineers, New York, NY., USA.

[15] ASME Boiler and Pressure Vessel Code, Section II, Part D, *Properties*, 2011, American Society of Mechanical Engineers, New York, NY., USA.

[16] Lam, P.S., Sindelar, R.L., Duncan, A.J., and Adams, T.M., 2014, "A Framework to Develop Flaw Acceptance

Criteria for Structural Integrity Assessment of Multipurpose Canisters for Extended Storage of Used Nuclear Fuel," Paper No. PVP2014-28990, Proceedings of ASME Pressure Vessels and Piping Conference, Anaheim, California, USA.

[17] API 579-1/ASME FFS-1, 2007, *Fitness-For-Service* (API 579 Second Edition), American Petroleum Institute, Washington, DC., USA.

[18] Bjorkman, G., Chuang, T.-J., Einziger, R., Malik, S, Malliakos, A., Mitchell, J, Navarro, C., Ryder, R., Shaukat, S., Ulses, A., and Zigh, G., 2007, *A Pilot Probabilistic Risk Assessment of a Dry Cask Storage System at a Nuclear Power Plant*, NUREG-1864, U.S. Nuclear Regulatory Commission Washington, DC., USA.

[19]*http://www.holtecinternational.com/productsandservices/wasteandfuelmanagement/multi-purpose-canisters/*

[20] Stoner, K.J., Sindelar, R.L, and Caskey, G.R., 1991, *Reactor Materials Program: Baseline Material Property Handbook — Mechanical Properties of 1950s Vintage Stainless Steel Weldment Components*, WSRC-TR-91-10, Westinghouse Savannah River Company, Aiken, South Carolina, USA.

[21] Milne, I, Ainsworth, R.A., Dowling, A.R., and Stewart, A.T., 1986, *Assessment of the Integrity of Structures Containing Defects*, Central Electricity Generating Board Report R/H/R6-Rev. 3, May 1986; Also in International Journal of Pressure Vessel & Piping, Vol. 32, pp. 3-104, 1988.

[22] Ainsworth, R.A., 1984, "The Assessment of Defects in Structures of Strain Hardening Materials," Engineering Fracture Mechanics, Vol. 19, pp. 633-642.

[23] Lam, P.S., 2000, *Comparison of Fracture Methodologies for Flaw Stability Analysis for High Level Waste Storage Tanks*, WSRC-TR-2000-00478, Westinghouse Savannah River Company, Aiken, South Carolina, USA.

[24] Lam, P.S., and Sindelar, R.L., 2004, "Comparison of Fracture Methodologies for Flaw Stability Analysis of Storage Tanks," in *Fracture Methodologies and Manufacturing*, *Processes,* Proceedings of ASME Pressure Vessels and Piping Conference, San Diego, California, PVP-Vol. 474, pp. 91-103.